DESIGN OF VISUAL NAVIGATION SYSTEM FOR AGRICULTURAL ROBOTS BASED ON PID-FUZZY CONTROL AND MONOCULAR VISION

/

基于 PID-模糊控制的单目视觉农田机器人视觉导航系统设计

Hanzhuo REN, Wei LI※), Shaobo YE, Bing XU 1)

College of Agricultural Engineering, Shanxi Agricultural University, Taigu 030801 / China;
Corresponding author: Wei LI
Tel: +86-0354-6288339; E-mail: jamesallenlw@163.com
DOI: https://doi.org/10.35633/inmateh-70-11

Keywords: *Monocular vision; Agricultural robots; Vision navigation system; PID-fuzzy control*

ABSTRACT

This study proposes a monocular vision navigation control system based on PID-fuzzy control, which travels along the edge of the path. It collects path image information through monocular vision, identifies the path edge through image processing to determine the preview point, and uses a combination of PID and fuzzy control to design a controller to track the preview point for path navigation. Coordinate calibration and conversion were performed on the monocular camera. According to the navigation strategy of driving along the edge of the path, the world coordinate equation of the path edge is obtained through image processing technology, and the preview point tracked by the navigation system is determined. The navigation parameters are determined based on the position of the preview point. The PID fuzzy controller system designed in this study can switch different control methods based on the position of the preview point. The verification results show that the average error of the navigation control system in tracking the path when driving in a straight line was 0.039 m, the average error when turning left was 0.079 m, and the average error when turning right was 0.121 m. The error range can meet the basic requirements of agricultural robot farmland operations. Research has shown that the navigation strategy based on PID-fuzzy joint controller to track the preview point along the path edge has a good effect on the visual navigation control system of agricultural robots.

摘要

本研究提出了一种沿路径边缘行驶，基于 PID-模糊控制的单目视觉导航控制系统，它通过单目视觉采集路径图像信息，图像处理识别路径边缘确定预瞄点，利用 PID 和模糊控制相结合的方式设计控制器跟踪预瞄点实现路径导航。首先对单目摄像机进行坐标标定与转换，实现了从图像坐标系到世界坐标系的坐标转换，并通过试验验证了标定结果的准确性。根据沿路径边缘行驶的导航策略，通过图像处理技术得到路径边缘的世界坐标方程，确定导航系统追踪的预瞄点，根据预瞄点的位置确定导航参数。本研究设计的 PID-模糊控制器系统，能够根据预瞄点的位置不同切换不同的控制方式。最终对该控制系统的单目视觉导航系统进行了试验验证，验证结果表明该导航控制系统在直线行驶时跟踪路径的平均误差是 0.039 m，左转弯时的平均误差为 0.079 m，右转弯平均误差 0.121 m，误差范围能够满足农业机器人农田作业的基本要求。研究表明，基于 PID-模糊联合控制器控制沿路径边缘追踪预瞄点行驶的导航策略对农田机器人视觉导航控制系统效果良好。

INTRODUCTION

Due to its affordable price, large amount of information available, and flexible guidance, visual navigation has become the fastest developing navigation strategy in recent years, and has also become a hot research topic for navigation strategies both domestically and internationally, with broad application prospects (*Zhang et al., 2022; Yang et al., 2022; Wang et al., 2021*). Robot visual navigation technology can usually be divided into indoor visual navigation and outdoor visual navigation. Generally speaking, the difficulty of outdoor robot visual navigation is much greater than that of indoor robot visual navigation, as indoor robots can achieve regular paths, uniform lighting, and less random interference (*Wang et al., 2022*; *Khan et al., 2022*). In addition to facing irregular paths and constantly changing light intensity, outdoor robot visual navigation also needs to face various interferences that may occur at any time (*Lai et al., 2023*).

Hanzhuo Ren, B.S. Stud. Eng.; Wei Li, Lecturer Ph.D. Eng.; Shaobo Ye, Lecturer Ph.D. Eng.; Bing Xu, Lecturer Ph.D. Eng.

Agricultural robot visual navigation belongs to outdoor visual navigation, and agricultural robots face complex agricultural environments, which further increases the difficulty of visual navigation (*Li et al., 2018; Tai J. et al., 2020*).

The earliest application of visual navigation technology to the agricultural field was Marr's visual Theory of computation in the 1970s. Europe, America and other countries took the lead in carrying out relatively in-depth research and exploration, and achieved certain results (*Li D. et al., 2017; Phalak Y. et al., 2018*). China's research in the field of agricultural robot visual navigation started relatively late and has achieved considerable research results through continuous research and exploration in recent years (*Ren et al., 2021*).

At present, there is no unified, effective and feasible solution for agricultural robot visual navigation technology, which focuses on researching specific navigation strategies for different agricultural environments (*Guan et al., 2020; Liu, 2019*). This article mainly proposes a visual navigation strategy for driving along the edge of a path in agricultural environments with obvious path edges.

The main contributions of this article are as follows:

(1) A visual navigation strategy for driving along the edge of the path is proposed. Due to the frequent need for agricultural robots to operate along the edge of the path in agricultural work environments, this paper proposes a visual navigation strategy for driving along the edge of the path.

(2) A PID-fuzzy controller has been designed, which can freely switch between PID control and fuzzy control methods. PID control has good stability and high accuracy, and fuzzy control guidance is flexible and suitable for nonlinear and complex control. The PID fuzzy controller combines the advantages of both controllers and can adapt well to the designed navigation strategy.

(3) The feasibility of the navigation strategy and the effectiveness of the controller design were verified through experiments. By conducting tests on the agricultural robot testing platform for straight, left turn, and right turn driving, the deviation of the agricultural robot's track from the predetermined track was measured, and a comprehensive evaluation of the navigation strategy and controller was conducted.

MATERIALS AND METHODS

Construction of agricultural robot test platform

The agricultural robot experimental platform mainly includes a frame, hub motor, hub motor controller, power supply, monocular camera, DSP image processing system, STM32 microcontroller, ultrasonic sensor, etc. The agricultural robot experimental platform controls the wheel hub motors of two front wheels for differential steering. The two rear wheels belong to a universal follower wheel and can rotate freely. The CCD camera is responsible for collecting image information and transmitting it to the DSP processor for processing. The DSP image processing controller model is DM642, mainly responsible for image information processing in monocular vision. DSP communicates with STM32 and transmits the DSP image processing results to the STM32 microcontroller. STM32 controls the wheel hub motor speed of the left and right front wheels for navigation based on image information and navigation algorithms. Ultrasonic sensors are mainly used to detect obstacles and achieve obstacle avoidance in agricultural robot testing platforms. Fig. 1 shows the overall structure of the agricultural robot experimental platform.

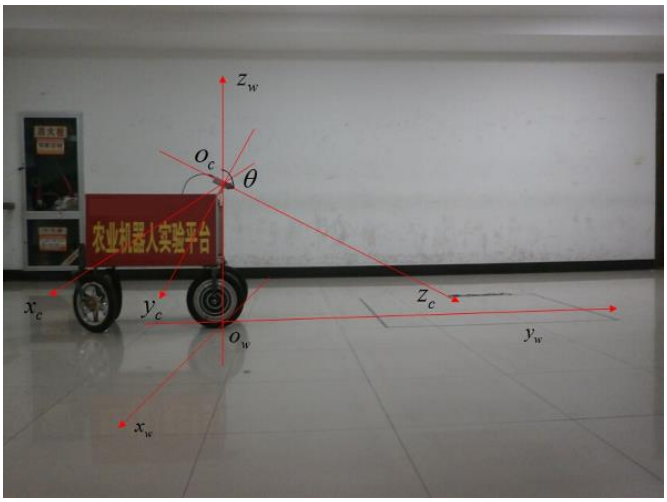

Fig. 1 - The overall structure of the agricultural robot experimental platform

Camera pixel calibration

Conversion relationship between different coordinate systems

The coordinates in the image information processed by the image processing system are the pixel coordinates of the image captured by the CCD camera, and for the navigation system to navigate correctly, it is necessary to use the world coordinate system for navigation (*Zeng et al., 2020*). Therefore, it is particularly important to convert the pixel coordinates of the image to world coordinates (*Liu Y., 2019*). Fig. 2 shows the relationship between different coordinate systems.

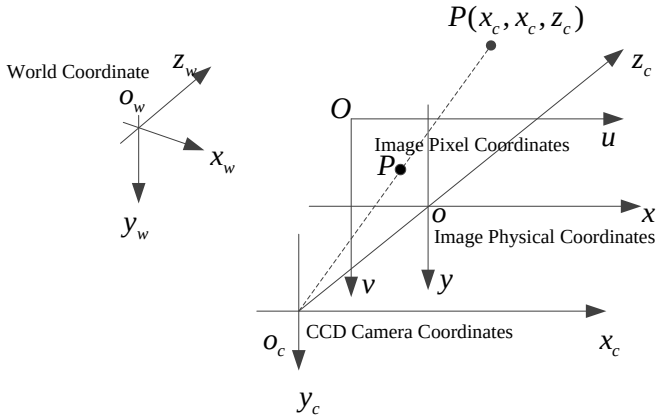

Fig. 2 - The relationship between different coordinate systems

Assuming the camera coordinate system rotates θ clockwise around the axis x_C, moving parallel along the x_C axis $-h_1$, moving parallel along the y_C axis $-h_2$, and moving parallel along the z_C axis $-h_3$ can obtain the world coordinate system. The relationship between the world coordinate system (x_w, y_w, z_w) and the camera coordinate system (x_c, y_c, z_c) is as follows:

$$\begin{bmatrix} x_c \\ y_c \\ z_c \\ 1 \end{bmatrix} = TR \begin{bmatrix} x_w \\ y_w \\ z_w \\ 1 \end{bmatrix} = \begin{bmatrix} 1 & 0 & 0 & -h_1 \\ 0 & \cos\theta & -\sin\theta & -h_2 \\ 0 & \sin\theta & \cos\theta & -h_3 \\ 0 & 0 & 0 & 1 \end{bmatrix} \begin{bmatrix} x_w \\ y_w \\ z_w \\ 1 \end{bmatrix} \tag{1}$$

where:

$$R = \begin{bmatrix} 1 & 0 & 0 & 0 \\ 0 & \cos\theta & -\sin\theta & 0 \\ 0 & \sin\theta & \cos\theta & 0 \\ 0 & 0 & 0 & 1 \end{bmatrix} \tag{2}$$

$$T = \begin{bmatrix} 1 & 0 & 0 & -h_1 \\ 0 & 1 & 0 & -h_2 \\ 0 & 0 & 1 & -h_3 \\ 0 & 0 & 0 & 1 \end{bmatrix} \tag{3}$$

The conversion relationship between the physical coordinate system of the image *(u, v)* and the pixel coordinates stored in the image processing system (x, y) is:

$$\begin{cases} u = u_0 + \dfrac{x}{s_x} \\ v = v_0 + \dfrac{y}{s_y} \end{cases} \tag{4}$$

Based on the above analysis, the final relationship between the pixel coordinates *(u, v)* of the image and the world coordinate system (x_w, y_w, z_w) is:

$$\begin{cases} u = u_0 + \dfrac{f}{s_x} \cdot \dfrac{x_w - h_1}{y_w \cdot \sin\theta + z_w \cdot \cos\theta - h_3} \\ v = v_0 + \dfrac{f}{s_y} \cdot \dfrac{y_w \cdot \cos\theta - z_w \cdot \sin\theta - h_2}{y_w \cdot \sin\theta + z_w \cdot \cos\theta - h_3} \end{cases} \quad (5)$$

where u_0 and v_0 are the camera internal parameters, [pixel number]. h_1, h_3 and h_3 are the distances the camera coordinate system moved along the x, y and z of the world coordinate system, [m]. θ is the camera coordinate system rotate clockwise angle around the x axis of the world coordinate system, [°].

Camera calibration test

The camera calibration process is as follows:

(1) Establish a world coordinate system and a camera coordinate system: The establishment of the world coordinate system is shown in Fig. 1, with the projection point of the camera center to the ground as the origin of the world coordinate system. The forward direction of the agricultural robot test platform is the positive direction of the Y-axis, the upward direction perpendicular to the ground is the positive direction of the Z-axis, and the direction perpendicular to the robot's forward direction and to the right is the positive direction of the X-axis. The camera coordinate system takes the camera optical center as the coordinate origin, with the positive direction of the Z axis along the camera, the positive direction of the Y axis perpendicular to the camera downwards, and the positive direction of the X axis perpendicular to the Y-Z axis plane to the right.

(2) The vertical distance between the optical center of the camera and the ground, measured as 0.85 m, is the angle between the Z axis of the camera coordinate system and the Z axis of the world coordinate system.

(3) Adjust the focal length of the camera to obtain the clearest ground image information and capture images. The world coordinates of the marked points on the ground can be obtained through measurement, and the pixel coordinates of the marked points in the collected image information can be obtained through image information processing.

(4) By incorporating the obtained world coordinates and image pixel coordinates into formula 5, the unknown parameters in the equation can be solved, thereby achieving camera calibration.

The Camera calibration test results is shown in Table 1.

Table 1

The result of camera calibration

Camera external parameters				Camera internal parameters		
h_1	h_2	h_3	θ	(u_0,v_0)	m	n
0.05	0.03	0.91	123	(309.71,242.31)	320.44	354.72

The final conversion relationship between the world coordinate system and the camera pixel coordinates is as formula (6):

$$\begin{cases} x_w = \dfrac{187.7 - 0.565u + 0.068v}{-231.5 - 0.54v} \\ y_w = \dfrac{992.0 - v}{231.5 + 0.54v} \end{cases} \quad (6)$$

where u and v are the camera pixel coordinate system, [pixel number]. x_w and y_w are the world coordinate system.

In order to verify the accuracy of formula (6), twenty points were randomly selected in the world coordinate system to find the corresponding pixel points in the image coordinate system. The world coordinates of the corresponding points in the world coordinate system were calculated using the pixel coordinates of the pixel points and the formula, and the error between the calculated and actual values of the world coordinates was compared. From the error analysis, it can be seen that the maximum error does not exceed 0.11 m, while most errors are mainly concentrated within the range of 0.07 m. Considering the complexity of the agricultural robot operating environment, this error is within the allowable range and can meet the accuracy requirements.

Driving strategy along the edge of the path

Agricultural robots mainly operate in agricultural environments, which are relatively complex. However, there are generally obvious path edges in farmland (*Peng et al., 2018*). Therefore, this article proposes a navigation strategy for agricultural robots to travel by path edges. The agricultural robot determines the world coordinates of the preview point based on the collected path information and the navigation strategy of driving along the edge of the path. Then, the controller controls the hub motor to track the position of the preview point, thereby achieving the navigation of the agricultural robot driving along the edge of the path. The driving strategy along the edge of the path is shown in Fig. 3.

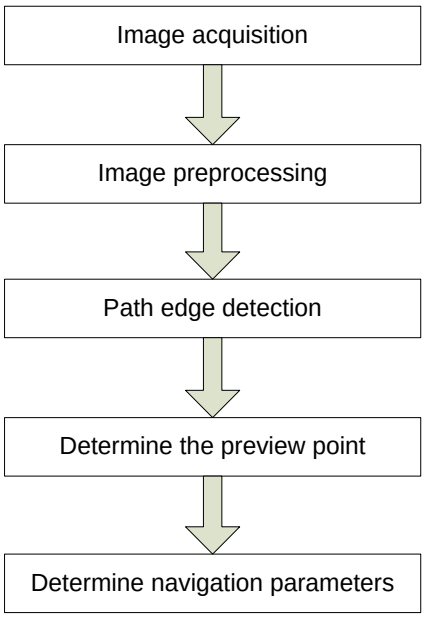

Fig. 3 - The driving strategy along the edge of the path

The image information collected by the camera needs to be preprocessed using DM642, which mainly includes image graying, threshold segmentation, morphological processing, edge detection, line detection, etc. The main image Processing process is shown in Fig. 4.

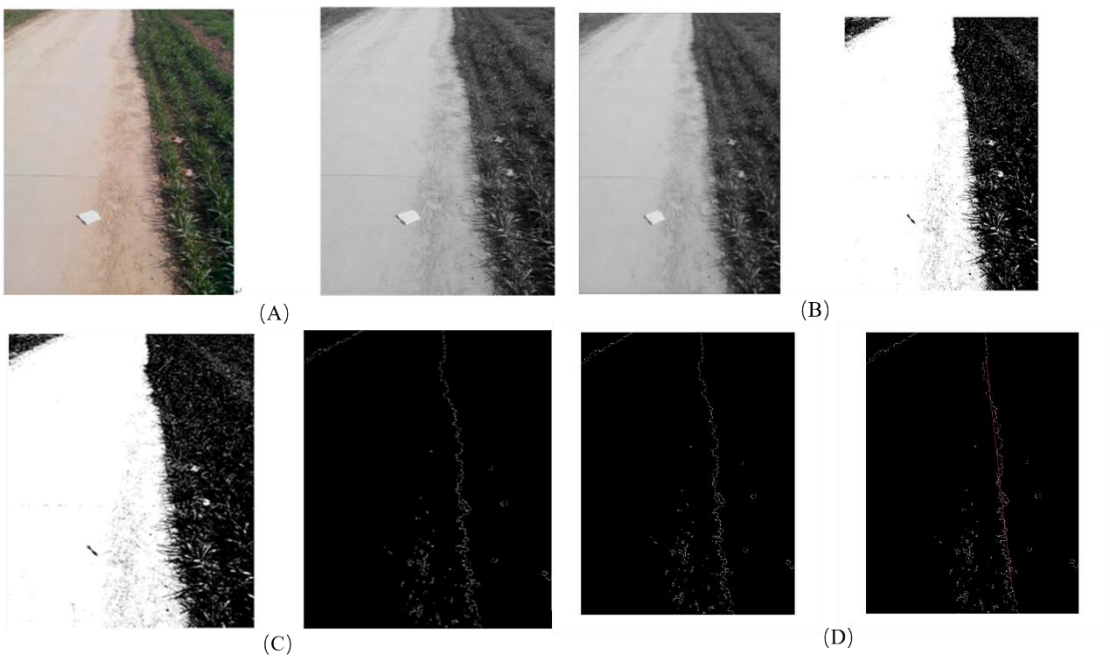

Fig. 4 - The image processing process

Finding the preview point for path tracking

Through the previous image processing, the path edge can be already found in the image and the path edge can be fit with a straight line to obtain the analytical equation of the path edge in the image. This expression is then transformed into the world coordinate system through coordinates, and the expression of the path edge in the world coordinate system is obtained. Then, based on the equation of the path edge in the world coordinate system and the width of the agricultural robot body, the preview point position for path tracking can be determined as the tracking target for navigation. Fig. 5 illustrates the main steps to determinate the preview point.

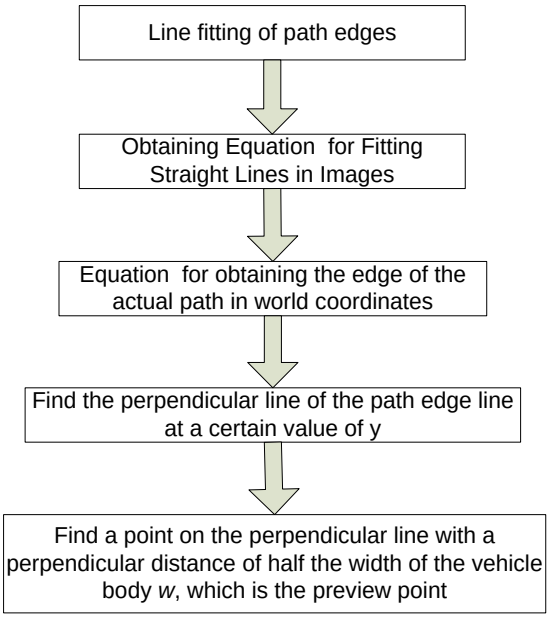

Fig. 5 - The determination of preview point

Assuming the linear equation of the navigation path edge in the pixel coordinate system is:

$$y = k_1 u + b_1 \tag{7}$$

The equation expression for the navigation path edge in the world coordinate system is:

$$y = k_2 x + b_2 \tag{8}$$

After determining the preview point, it is necessary to design a controller to control the agricultural robot experimental platform to track the constantly changing preview point. Navigation parameters that describe the position of the preview point need to be defined.

As shown in Figure 11, the navigation parameters mainly include the following three: preview point lateral offset *d*, path tangent direction angle φ, and preview point direction deviation angle *θ*. The preview point lateral offset *d* refers to the distance between the tracked preview point position and the world coordinate system y axis, while the path tangent direction angle *θ* refers to the angle between the direction of the path edge fitting line and the positive direction x in the world coordinate system. The directional deviation angle φ refers to the angle between the line connecting the tracked preview point position and the world coordinate origin and the world coordinate system y axis.

It should be pointed out that when the tracked preview point position is in the first quadrant of the world coordinate system, the deviation angle φ and the lateral offset *d* of the preview point are both positive, while when the tracked preview point position is in the second quadrant of the world coordinate system, the deviation angle φ and the lateral offset d of the preview point are both negative. During the process of changing the position of the preview point from the first phenomenon to the second quadrant, the tangent angle of the path direction changes from 0° to 180°. The navigation parameters' calculation process are showed in the Tab. 2.

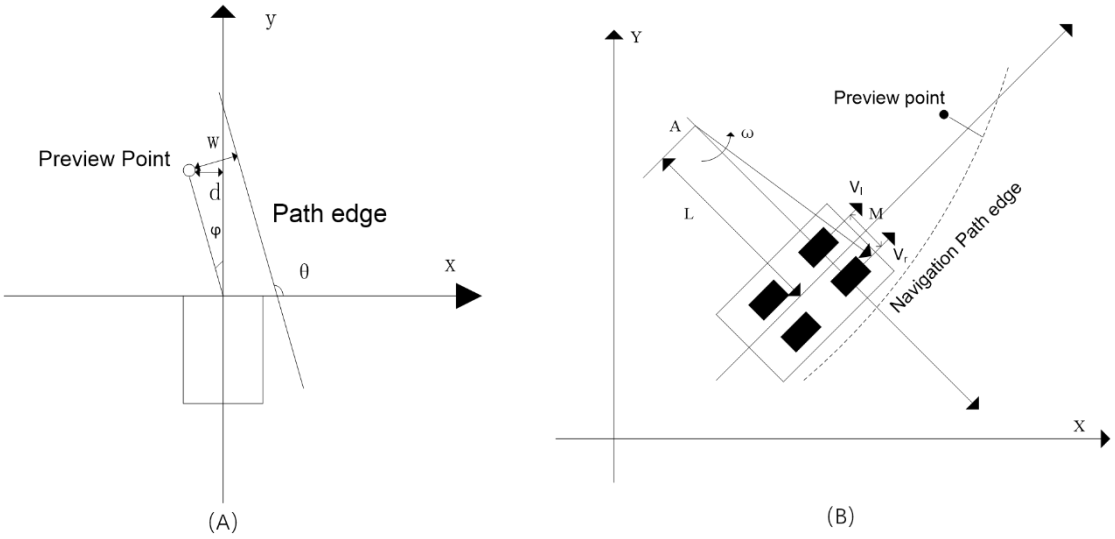

Fig. 6 - Navigation parameter diagram
(A) Straight line path; (B) Curve path

Table 2

Determination of navigation parameters in different situations

Navigation parameter	$0.5 \le \lvert k_2 \rvert \le 300$	$\lvert k_2 \rvert > 300$	$\lvert k_2 \rvert < 0.5$
d	$1-b_2-\frac{wk_2^{\ 2}}{\sqrt{k_2^{\ 2}+1}}$	$b-w$	$\begin{cases} l+w-n_1 (x_1>0) \\ w+n_1-l (x_1<0) \end{cases}$
φ	$\arctan\frac{x}{y}$	$\arctan\frac{b-w}{l}$	$\begin{cases} \arctan\frac{l+w-n_1}{n_1+w} (x_1>0) \\ \arctan\frac{w+n_1-l}{n_1-w} (x_1<0) \end{cases}$
θ	$\begin{cases} \arctan k_2 (k_2>0) \\ \pi+\arctan k_2 (k_2<0) \end{cases}$	90	$\begin{cases} 0 \quad (x_1>0) \\ 180 (x_1<0) \end{cases}$

Assuming that the direction deviation generated by the agricultural robot test platform after time Δt, that is, the defined path tangent deviation angle θ=Δe_θ, and the generated lateral deviation distance $d = \Delta e_d$, then the Kinematics equation of the agricultural robot test platform can be expressed as follows:

$$\begin{aligned} \frac{\Delta e_\theta}{\Delta e_t} &= \omega = \frac{v_r + v_l}{2L} \\ \frac{\Delta e_d}{\Delta e_t} &= \frac{v_r + v_l}{2} \cdot \sin \Delta e_\theta \end{aligned} \tag{9}$$

where: v_l and v_r are the speeds of left and right wheels, respectively, [m/s]; L is the width of the experimental platform vehicle, [m]; e_θ is the defined path tangent deviation angle, [°]; e_d is the generated lateral deviation distance, [m]; e_t is an extremely short running time, [s].

The kinematics equation of the agricultural robot test platform can be simplified as follows:

$$\begin{aligned} \dot{e}_\theta &= \omega = \frac{v_r + v_l}{2L} \\ \dot{e}_d &= \frac{v_r + v_l}{2} \cdot \sin \Delta e_\theta \end{aligned} \tag{10}$$

Let $v_c = \frac{v_r + v_l}{2L}$.

In this way, the Kinematics equation of the agricultural robot test platform can be further simplified as:

$$\begin{bmatrix} \dot{e}_d \\ \dot{e}_\theta \end{bmatrix} = \begin{bmatrix} 0 & v_c \\ 0 & 0 \end{bmatrix} \begin{bmatrix} e_d \\ e_\theta \end{bmatrix} + \begin{bmatrix} 0 \\ \frac{1}{L} \end{bmatrix} (v_c) + \begin{bmatrix} \Delta_d \\ \Delta_\theta \end{bmatrix} \quad (11)$$

Fuzzy control can achieve control of the controlled object without an accurate model of the controlled object. Fuzzy control can simulate human preview control behavior, especially in the absence of an accurate model of the controlled object, and can achieve good control effects in complex environments such as nonlinearity. The working environment of agricultural robots is generally complex, and choosing a fuzzy controller can adapt to this complex environment.

Fuzzy controllers have their own shortcomings, such as poor stability and difficulty in eliminating static errors. While, classical PID controllers can effectively solve these problems. Therefore, this controller chooses a control method that combines PID control and fuzzy control. When the path turns or the deviation distance of the preview point is large, a robust fuzzy controller is selected, PID controller is chosen in areas where the deviation distance between the straight path or the preview point is small. This can combine the advantages of two control methods, which can meet the stability and robustness demand of the controller.

RESULTS

To verify the tracking effect of the proposed navigation strategy on the agricultural robot test platform on different paths, three types of tracks have been set up, including straight line, left turn, and right turn. The travel trajectory errors of the agricultural robot have been measured. The experimental testing process is shown in Fig. 7.

Fig. 7 - Driving trajectory test

(A) Strait line test; (B) Turn left test; (C) Turn right test; (D) Error data measurement; (E) Driving trajectory leakage bottle; (F) Obstacle avoidance test

The average error of tracking the straight line path is 0.039 m, the average error of left turn is 0.079 m, and the average error of right turn is 0.121 m (Fig. 8).

Considering that the agricultural robot works in an agricultural environment, these errors are not too large, usually within the allowable range. The mean squared error of straight line driving is 0.036 m, the mean squared error of left turn tracking is 0.059 m, and the mean squared error of right turn tracking is 0.070 m.

The mean squared error of straight line driving is significantly smaller than that of left turn and right turn, and the mean squared error of straight line driving is also smaller than that of left turn and right turn. This is because straight line driving uses PID controllers, while left and right turns combines PID and fuzzy control, and PID control accuracy and stability are significantly better than fuzzy control. Fuzzy control can adapt well to complex control with high nonlinearity such as left and right turns, and has good guidance flexibility.

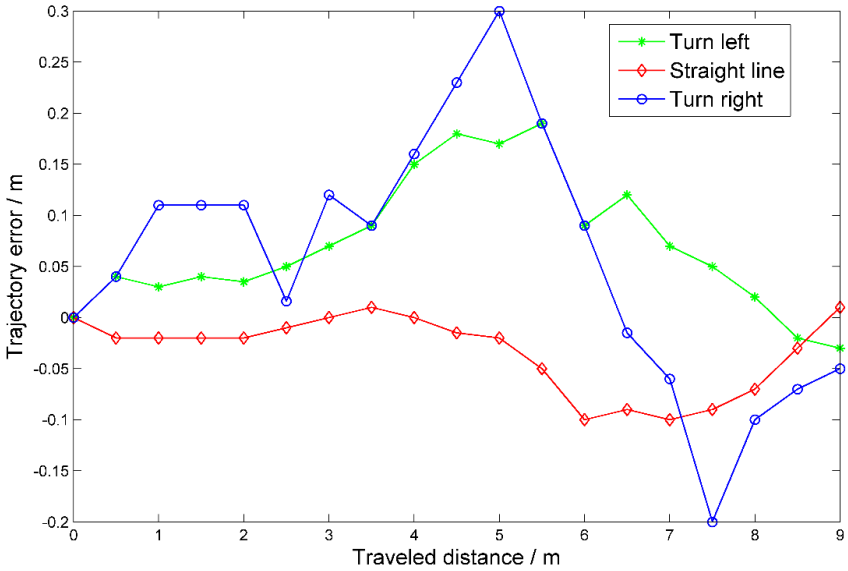

Fig. 8 - Trajectory error curve

CONCLUSIONS

The visual navigation system of the agricultural robot experimental platform was tested by simulating farmland paths. The experimental results show that the agricultural robot experimental platform can accurately track the edges of straight and curved paths on a flat football field, and be able to independently achieve turning path tracking control. When the path is lost, the agricultural robot experimental platform can automatically deflect to the right to find the edge of the path, so it has a certain degree of fault tolerance for short-term path loss. In addition, the ultrasonic sensor module of the agricultural robot testing platform was tested. When encountering obstacles, the agricultural robot testing platform can stop in a timely manner to prevent danger. The driving trajectory of the agricultural robot test platform is relatively smooth, and there are certain overshoots and oscillations in the system during the driving process. Given that the agricultural environment does not require high navigation accuracy, the proposed monocular vision PID-fuzzy navigation strategy can basically meet the design requirements to drive along the edge of the path.

ACKNOWLEDGEMENTS

This research, titled “Design of Visual Navigation System for Agricultural Robots Based on PID-Fuzzy Control and Monocular Vision”, was funded by project: “Design of Ultrasonic Generator and its Application in Facility planting (Grant No. 2016010)”, and project “Study on Detection of organophosphorus Pesticide residues based on Electrochemical biosensor (Grant No. 2022BQ35)”.

REFERENCES

[1] Guan Z.H., Chen K.Y., Ding Y.C., Wu C.Y., Liao Q.X., (2020), Visual navigation path extraction method in rice harvesting, *Transactions of the Chinese Society for Agricultural Machinery*, vol.51, Issue 1, pp.19-28;

[2] Khan D., Cheng Z., Uchiyama H., et al., (2022), Recent advances in vision-based indoor navigation: A systematic literature review, *Computers & Graphics*, Vol.104, pp.24-45, Elsevier, London / England;

[3] Lai H.R., Zhang Y.W., Zhang B., et al., (2023), Design and experiment of the visual navigation system for a maize weeding robot (玉米除草机器人视觉导航系统设计与试验), *Transactions of the Chinese Society of Agricultural Engineering*, Vol.39, Issue 01, pp.18-27, Beijing / China.

[4] Li Y.W., Xu J.J., Wang M.F., et al., (2019), Development of autonomous driving transfer trolley on field roads and its visual navigation system for hilly areas, *Transactions of the Chinese Society of Agricultural Engineering*, Vol. 35, Issue 01, pp.52-61, Beijing / China.

[5] Li D., Xu S., Zheng Y., (2017), Navigation Path Detection for Cotton Field Operator Robot Based on Horizontal Spline Segmentation. *International Journal of Information Technology & Web Engineering*, Vol.12, Issue 3, pp.28-41, USA;
[6] Liu B., (2019), *Research on visual navigation system of citrus picking robot mobile platform, MSc dissertation*, Chongqing University of Technology, Chongqing / China;
[7] Liu Y., Gao G.Q., (2019), Recognition of visual navigation directrix between winter fruit tree row, *Journal of Chinese Agricultural Mechanization*, vol.40, Issue 5, pp.160-166, China;
[8] Peng S.Z., Li J.B., (2018), Design and implementation of jujube garden visual navigation path extraction software, *Jiangsu Agricultural Sciences*, vol.46, Issue 10, pp.213-217;
[9] Phalak Y., Charpe G., Paigwar K., (2018), Omnidirectional Visual Navigation System for TurtleBot Using Paraboloid Catadioptric Cameras. *Procedia Computer Science*, Vol.133, pp.190-196, Netherlands;
[10] Ren X.D., Wang H.C., Shi X., et al., (2021), Research on visual navigation path detection method for dense plum grove, *INMATEH - Agricultural Engineering*, Vol.65, Issue 3, PP. 111-118, Romania;
[11] Tai J., Li H.T., Du Y.F, Mao E.R., Zhang J.N., Long X.J., (2020), Rapid design of maize ear harvester header based on knowledge engineering. *INMATEH - Agricultural Engineering*, Vol.61, Issue 2, pp.263-272, Romania;
[12] Wang T., Chen B., Zhang Z., et al., (2022), Applications of machine vision in agricultural robot navigation: A review, *Computers and Electronics in Agriculture*, Vol. 198, 107085, Ed. Elsevier, London/England;
[13] Wang Z., Cheng X., (2021), Adaptive optimization online IMU self-calibration method for visual-inertial navigation systems, *Measurement*, Vol.180, 109478, Ed. Elsevier, London / England;
[14] Yang Z., Ouyang L., Zhang Z. et al., (2022), Visual navigation path extraction of orchard hard pavement based on scanning method and neural network, *Computers and Electronics in Agriculture*, Vol.197, 106964, Ed. Elsevier, London / England;
[15] Zeng H.W., Lei Z.B., Tao J.F., Zhang W., Liu C.L., (2020), Navigation line extraction method for combine harvester under low contrast conditions, *Transactions of the Chinese Society of Agricultural Engineering*, vol.36, Issue 4, pp.18-25;
[16] Zhang T.Y., Hu X.G., Xiao J. et al., (2022), A survey of visual navigation: From geometry to embodied AI, *Engineering Applications of Artificial Intelligence*. Vol.114, 105036, Ed. Elsevier, London / England;